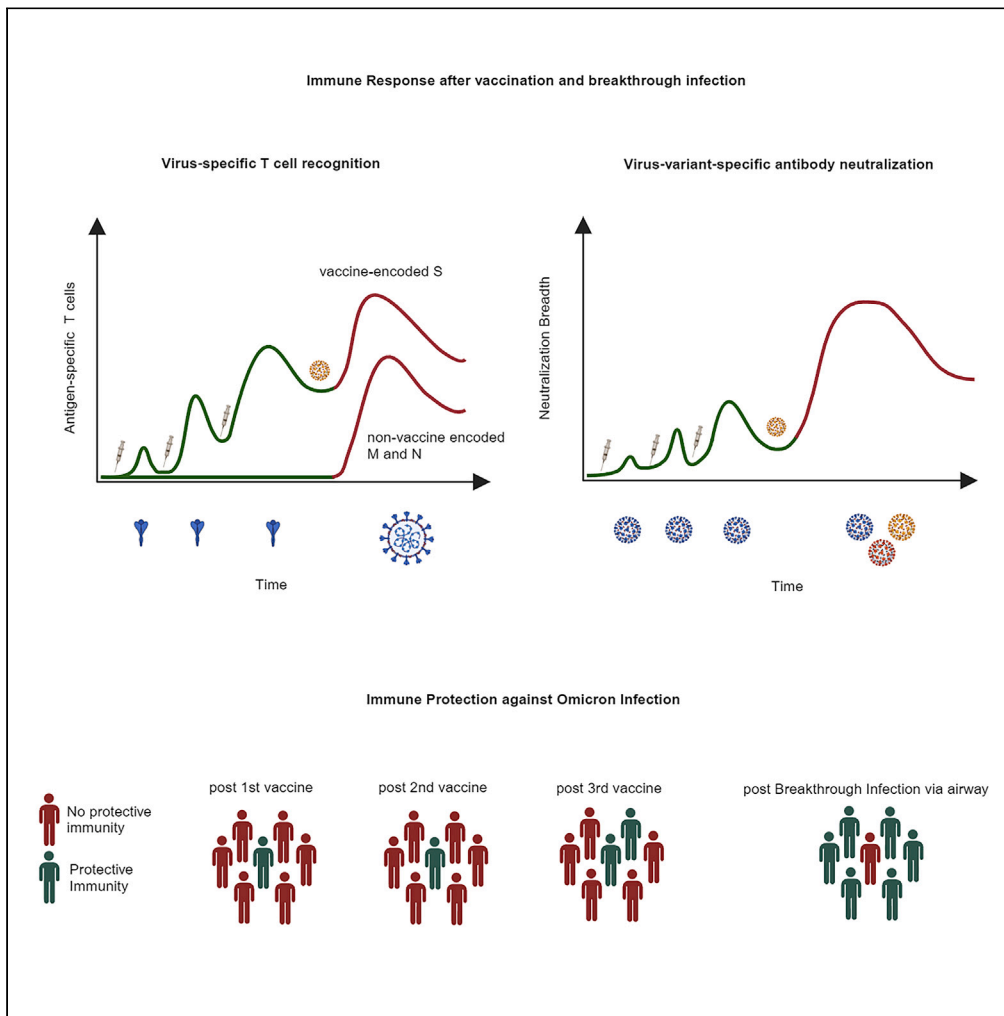# iScience

Article

Evolution of protective SARS-CoV-2-specific B and T cell responses upon vaccination and Omicron breakthrough infection

Mohamed I.M. Ahmed, Sebastian Einhauser, Clemens Peiter, ..., Ralf Wagner, Christof Geldmacher, on behalf of the KoCo19/ ORCHESTRA working group

geldmacher@lrz.uni-muenchen. de

Highlights

High level of protection from re-infection after Omicron breakthrough infection

Higher neutralization titers reduce hazard for Omicron (re)-infection

Modeling shows lower viral loads during re-infection with a new virus variant

BTI-induced immunity likely reduced virus transmission in Bavarian winter 22/23

Article

Evolution of protective SARS-CoV-2-specific B and T cell responses upon vaccination and Omicron breakthrough infection

Mohamed I.M. Ahmed,[1,2] Sebastian Einhauser,[3] Clemens Peiter,[4] Antonia Senninger,[3] Olga Baranov,[1,2] Tabea M. Eser,[1,2,5] Manuel Huth,[4,6] Laura Olbrich,[1,2] Noemi Castelletti,[1] Raquel Rubio-Acero,[1] George Carnell,[7] Jonathan Heeney,[7] Inge Kroidl,[1,2] Kathrin Held,[1,2] Andreas Wieser,[1,2,5] Christian Janke,[1] Michael Hoelscher,[1,2,5,8] Jan Hasenauer,[4,6,9,11] Ralf Wagner,[3,10,11] Christof Geldmacher,[1,2,5,11,12,*] and on behalf of the KoCo19/ORCHESTRA working group

SUMMARY

Severe acute respiratory syndrome coronavirus 2 (SARS-CoV-2) Omicron breakthrough infection (BTI) induced better protection than triple vaccination. To address the underlying immunological mechanisms, we studied antibody and T cell response dynamics during vaccination and after BTI. Each vaccination significantly increased peak neutralization titers with simultaneous increases in circulating spike-specific T cell frequencies. Neutralization titers significantly associated with a reduced hazard rate for SARS-CoV-2 infection. Yet, 97% of triple vaccinees became SARS-CoV-2 infected. BTI further boosted neutralization magnitude and breadth, broadened virus-specific T cell responses to non-vaccine-encoded antigens, and protected with an efficiency of 88% from further infections by December 2022. This effect was then assessed by utilizing mathematical modeling, which accounted for time-dependent infection risk, the antibody, and T cell concentration at any time point after BTI. Our findings suggest that cross-variant protective hybrid immunity induced by vaccination and BTI was an important contributor to the reduced virus transmission observed in Bavaria in late 2022 and thereafter.

INTRODUCTION

The emergence and dominance of the severe acute respiratory syndrome coronavirus 2 (SARS-CoV-2) Omicron variant, in late 2021, resulted in high infection rates across populations with high vaccination coverage.[1,2] In Germany, roughly 63% of the population was vaccinated by summer 2021 and then boosted in autumn/winter 2021.[3] Likewise, a large proportion of the Bavarian population and in particular health care workers started SARS-CoV-2 vaccinations in the first half of 2021 and were boosted with a third RNA vaccination between October and December 2021, just before the emergence of Omicron in Bavaria.[1] Despite the high vaccination rates, SARS-CoV-2 Omicron rapidly replaced Delta by efficiently spreading among vaccinated individuals during multiple waves until December 2022, albeit having a lower risk of severe COVID-19.[4,5] Since then, the reported case numbers substantially declined and remained on a comparatively low level as of beginning of 2023.[6]

Parameters defining protective immunity to Omicron are likely comparable to those established in the pre-Omicron era; neutralizing antibody titers positively correlated with protection from SARS-CoV-2 infection.[7–10] Antibody transfer using spike (S)-specific immunoglobulin G (IgG) was sufficient to mediate protection from SARS-CoV-2 infection in a preclinical infection model.[9] We have recently reported that nucleocapsid (N)-specific T cell responses associated with control of primary SARS-CoV-2 infection in the upper airways before antibody seroconversion.[11] Moreover, memory T cells mediated protection from infection in several preclinical models; vaccine-induced airway-tissue-resident

[1]Division of Infectious Diseases and Tropical Medicine, University Hospital, LMU Munich, 80799 Munich, Germany
[2]German Centre for Infection Research (DZIF), Partner Site Munich, Munich, Germany
[3]Institute for Medical Microbiology and Hygiene, University of Regensburg, 93053 Regensburg, Germany
[4]Faculty of Mathematics and Natural Sciences, University of Bonn, 53113 Bonn, Germany
[5]Fraunhofer Institute for Translational Medicine and Pharmacology ITMP, Immunology, Infection and Pandemic Research, 80799 Munich, Germany
[6]Institute of Computational Biology, Helmholtz Zentrum München – German Research Center for Environmental Health, 85764 Neuherberg, Germany
[7]Lab of Viral Zoonotics, Department of Veterinary Medicine, University of Cambridge, Cambridge, UK
[8]Unit Global Health, Helmholtz Zentrum München, German Research Center for Environmental Health (HMGU), 85764 Neuherberg, Germany
[9]Center for Mathematics, Technische Universität München, 85748 Garching, Germany
[10]Institute of Clinical Microbiology and Hygiene, University Hospital Regensburg, 93053 Regensburg, Germany
[11]These authors contributed equally
[12]Lead contact
*Correspondence: geldmacher@lrz.uni-muenchen.de
https://doi.org/10.1016/j.isci.2024.110138

T cells targeting the N protein protected mice upon SARS-CoV-1 challenge.[12] Similarly, intranasal vaccination with N and membrane protein (M, both are structural proteins of the virion)-encoding vectors induced protective T cell responses in a non-human primate model.[13] Indeed, accumulating evidence suggests that SARS-CoV-2-specific T cell responses contribute to control of infection.[14–16] Furthermore, intramuscular vaccinations followed by breakthrough infection (BTI) result in a state of "hybrid immunity," characterized by high S-specific antibody responses, broadening of virus-specific T cell responses to non-vaccine-encoded antigens, and formation of virus-specific T cell memory in the airway epithelium.[17–19] Yet, while BTI induces a high degree of protective immunity, the adaptation of antibody and T cell responses after BTI and their contribution to reduce infection spread within the population and development of further waves are incompletely understood. We therefore investigated the dynamics of SARS-CoV-2-variant-specific neutralizing antibody and T cell responses against vaccine-encoded and non-encoded viral antigens during vaccination, as well as before and after Omicron BTI spanning the transition from the pandemic to endemic phase (February 2021 to December 2022). Mathematical modeling was then used to assess the protective effect of antibody and T cell responses upon hypothetical re-exposure to neutralization-sensitive and neutralization-resistant SARS-CoV-2 variants, respectively.

RESULTS

Study population

To study vaccine-induced SARS-CoV-2-specific antibody and T cell responses, adult participants ($n = 50$) were recruited from Munich and surrounding regions in Bavaria, Germany. Figure 1 and Table 1 summarize the characteristics of the study population including vaccination types, SARS-CoV-2 infection events, and the observation time for each individual and also shows the concurrent SARS-CoV-2 incidence in Bavaria over the study period (February 2021 to December 2022). The median age was 31 years (range 21–57 years), and 68% (34/50) were female. Out of 50 individuals, no one reported chronic illnesses. 18 were recruited before their first vaccination, 23 before administration of the second vaccination, and an additional 9 participants were recruited after the second vaccination dose. 34 subjects (indicated in the underlying data) were followed longitudinally over an extended period from the first quarter of 2021 until December 2022. 16 participants were followed only for a limited time ($n = 7$) or lost to follow-up before receiving a third vaccination ($n = 9$). mRNA vaccines accounted for the majority of first immunizations, followed by adenoviral vector vaccines. Second and third booster vaccines were almost exclusively mRNA vaccines. Of these 34 vaccinated subjects, 33 were subsequently SARS-CoV-2 infected between November 2021 and December 2022 with a median time of 157.5 days after the last vaccination (range: 10–406 [days]). 31 of 33 individuals received three vaccinations and then were infected, while two participants were infected after the second vaccination. Infecting SARS-CoV-2 variants were determined by imputation, using the Bavarian Variants of Concern (Bay-VOC) database. One individual was determined to be infected with Delta, eight subjects with Omicron BA.1, 17 subjects with Omicron BA.2, and 14 were imputed to be infected with BA.5 or BA.5 sub-lineages. All infections induced N-specific antibody seroconversion (Figure S1, source data provided), and none were associated with hospitalization.

97% (30/31) of triple-vaccinated study participants, who were followed up until December 2022, experienced a BTI within 14 months of their last vaccination, while only four of these became infected a second time during the third and fourth quarter of 2022. Omicron BTI protected with a high efficiency of 88% (30 out of 34) from a second infection by December 2022 (Figure 1). When limiting the observation time to 230 days after three vaccinations or BTI, a difference can be observed where the majority vaccinated were infected thereafter. However, after this BTI, only one subject was reinfected a second time within 230 days of the first BTI (Figure 2).

SARS-CoV-2 neutralizing antibody and T cell response dynamics during vaccination

We assessed the dynamics of SARS-CoV-2 neutralizing activity against three clinically relevant variants of concern (VOCs) by determining the neutralizing antibody titers (half-maximal inhibitory concentration, IC_{50}) against Wuhan, Delta, and Omicron BA.5 (Figures 3A–3C, source data provided). The median, interquartile ranges, and number of tested subjects are provided for all study visits grouped in time bins (Table S1). Neutralizing antibody responses against all three variants followed a similar dynamic pattern, albeit at different intensity. IC_{50} values for Wuhan neutralization were consistently higher as compared to Delta or Omicron BA.5, whereas Delta and Omicron BA.5 neutralization was comparable after vaccination (Table S1). Each vaccination induced a peak response that was at least 11- to 21-fold higher compared to the last measured time point before vaccination (Table S1). Beyond 150 days after the second vaccination, titers had waned to pre 2nd vaccination levels, while the third vaccination boosted median IC_{50} titers 10- to 15-fold (depending on the tested variant) and remained significantly higher beyond 150 days as compared to the levels after the second vaccination for all tested variants ($p < 0.001$, $n = 10$, excluding participants with BTI before 3rd vaccination). We next wanted to assess neutralization breadth for different variants and combined single-variant data using a magnitude-breadth analysis approach,[18,19] in which areas under the curve (AUCs) were determined for every single serum sample, based on the neutralization data against all three variants. A slight, but statistically significant, increase in neutralization magnitude breadth was observed after each vaccination, dwindling quickly within 90 days (Figure 3D).

Next, we assessed the dynamics of T cell responses against the vaccine-encoded spike (S) and the non-vaccine-encoded nucleocapsid (N) and membrane (M) antigens (source data provided). Representative gating for CD4+ or CD8+ interferon (IFN) γ+ T cells is shown in Figure S2. 31%, 72%, and 94% of vaccinees had detectable S-specific T cell responses after the first, second, and third vaccination, respectively, and median frequencies of circulating S-specific CD4+ T cells increased from a median of 0.002% of CD4 T cells at baseline to 0.006% at 8–35 days after the 1st vaccination, and to 0.017% and 0.032% at 8–35 days after the 2nd and 3rd vaccination, respectively, and slightly declined thereafter (Figure 4A). Frequencies of circulating S-specific CD8+ T cells followed a similar dynamic pattern (Figure 4B), albeit with overall fewer IFNγ+ cells.
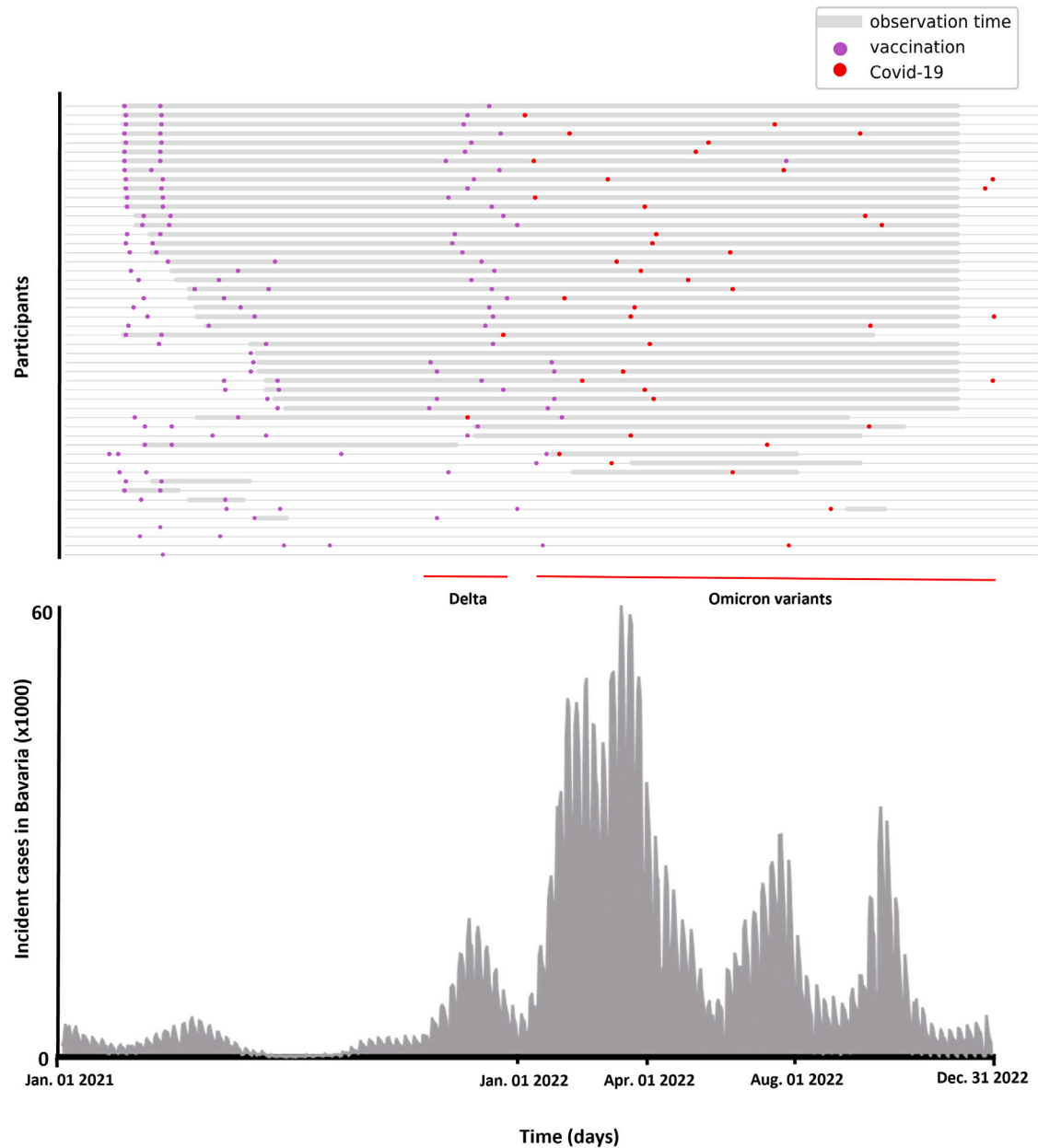
Figure 1. Overview of the study observation period, vaccination, and infection events for each study participant

Each line represents events for one participant from February 2021 until December 2022. The thicker gray lines indicate the study observation period, where there was active blood sampling, with vaccination dates (purple) and SARS-CoV-2 infection dates (red) indicated by dots (upper panel). SARS-CoV-2 incidence (x1000) in the study area (Bavaria, Germany) plotted over time (lower panel) for the same time period, with the delta and omicron waves indicated (www.lgl.bayern.de). A flowchart of the blood sampling process is shown in Figure S7.

BTI induces persisting high levels of cross-neutralizing antibody responses and T cell reactivity to structural proteins of the virion

Next, we assessed how BTI affected neutralization of the three tested SARS-CoV-2 variants and of spike, nucleocapsid, and membrane-specific T cell responses. BTI induced a 1.5- to 3.3-fold increase in IC_{50} values (depending on the variant) compared to peak levels at 8 to 35 days after the third vaccination. Neutralization remained high beyond 150 days (Figures 3A–3C; Table S1); even beyond 150 days after BTI, median IC_{50} neutralization values were comparable to peak levels directly after the third vaccination for all three tested variants. Like-wise, the BTI increased the magnitude breadth by a substantial degree (2-fold, $p < 0.0001$, Figure 3D), resulting in a sustained response for at least 150 days, exceeding what has been observed during the same time frame, after the third vaccination (2-fold, $p = 0.052$). The

Table 1. Basic characteristics of study population

n	50
Sex %	
Male	32% (16/50)
Female	68% (34/50)
Median age (range)	30 (21–57)
Vaccination 1 (B/M/A/J)[a]	32/1/11/6
Vaccination 2 (B/M/A/J)[a]	40/6/1/0
Vaccination 3 (B/M/A/J)[a]	31/9/0/0
Vaccination 4 (B/M/A/J)[a]	2/0/0/0
Median time between vaccination and infection (days, range)	157.5 (10–406)
Median time between last blood draw and infection (days, IQR range)	50 (52, 27–79)
Infection strain (Imputed)[c] (D/BA. 1/2/5/BQ. 1)[b]	1/8/17/13/1

[a]B = BioNTech, M = Moderna, A = AstraZeneca, J = Janssen.
[b]D = Delta strain, BA.1/2/5/BQ.1 = Omicron BA.1, BA.2, BA.5, BQ.1 strain.
[c]Imputed using the infection date and the Bay-VOC database. The strain with the highest likelihood is presented here.

longitudinal IC_{50} values against the three variants tested (Wuhan, Delta, and Omicron BA.5) for the 34 subjects followed up are shown in Figure S3.

Omicron BTI also boosted S-specific $CD4^+$ T cell frequencies up to a median of 0.041% after BTI (at 8–35 days, Figure 4, Table S2), which persisted beyond 150 days at 11-fold higher median compared to pre-vaccination levels. Simultaneously, S-specific $CD8^+$ T cells increased after BTI (Figure 4B), confirming our previous results from the pre-Omicron era.[18] Moreover, peak frequencies of vaccine-induced S-specific $CD8^+$ T cells after the 3rd vaccination are strongly correlated with post-BTI frequencies; at 8–35 days: r = 0.8, $p < 0.0001$; at 36–90 days: r = 0.5, $p < 0.04$; and >150 days: r = 0.7, $p = 0.01$ (Figure S4). Similar associations were also found for S-specific $CD4^+$ T cell responses (8–35 days: r = 0.4, $p = 0.03$ and >150 days: r = 0.6, $p = 0.02$, Figure S4). BTI elevated $CD4^+$ T cell responses targeting the non-vaccine-encoded nucleocapsid from background frequencies of 0.002% (median) at baseline to 0.025% at 8–35 days post-BTI (Figure 5A). In 17 of 18 participants, N-specific $CD4^+$ T cell responses remained above median baseline frequency beyond 150 days after BTI (Figure 5A, Table S2). Similar patterns were observed for N-specific $CD8^+$ T cells and membrane-specific T cell responses (Figures 5B–5D). These results show that Omicron BTI was
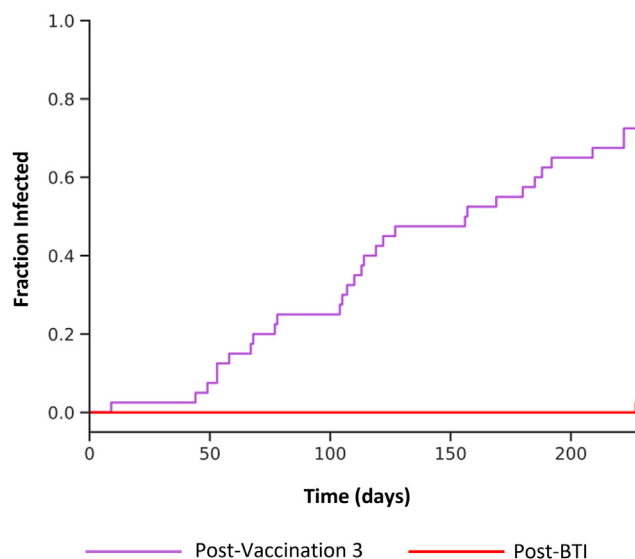

Figure 2. Cumulative incidence of SARS-CoV-2 infections after 3 vaccinations and after breakthrough infection
Kaplan-Meier survival analysis of incident (re-)infections was performed for 230 days after receiving the third vaccine dose (purple line, n = 32) and after the first BTI (red line, n = 18). Only subjects who have been observed for at least 230 days post 3rd vaccination or BTI were included in the plot. The limit of 230 days shown in the figure was set to retain sufficient number of subjects in the BTI group. Until 31st of December 2022, an additional 13 incident infections after third vaccination and 3 re-infections in the BTI group were recorded after 230 days and are not shown.
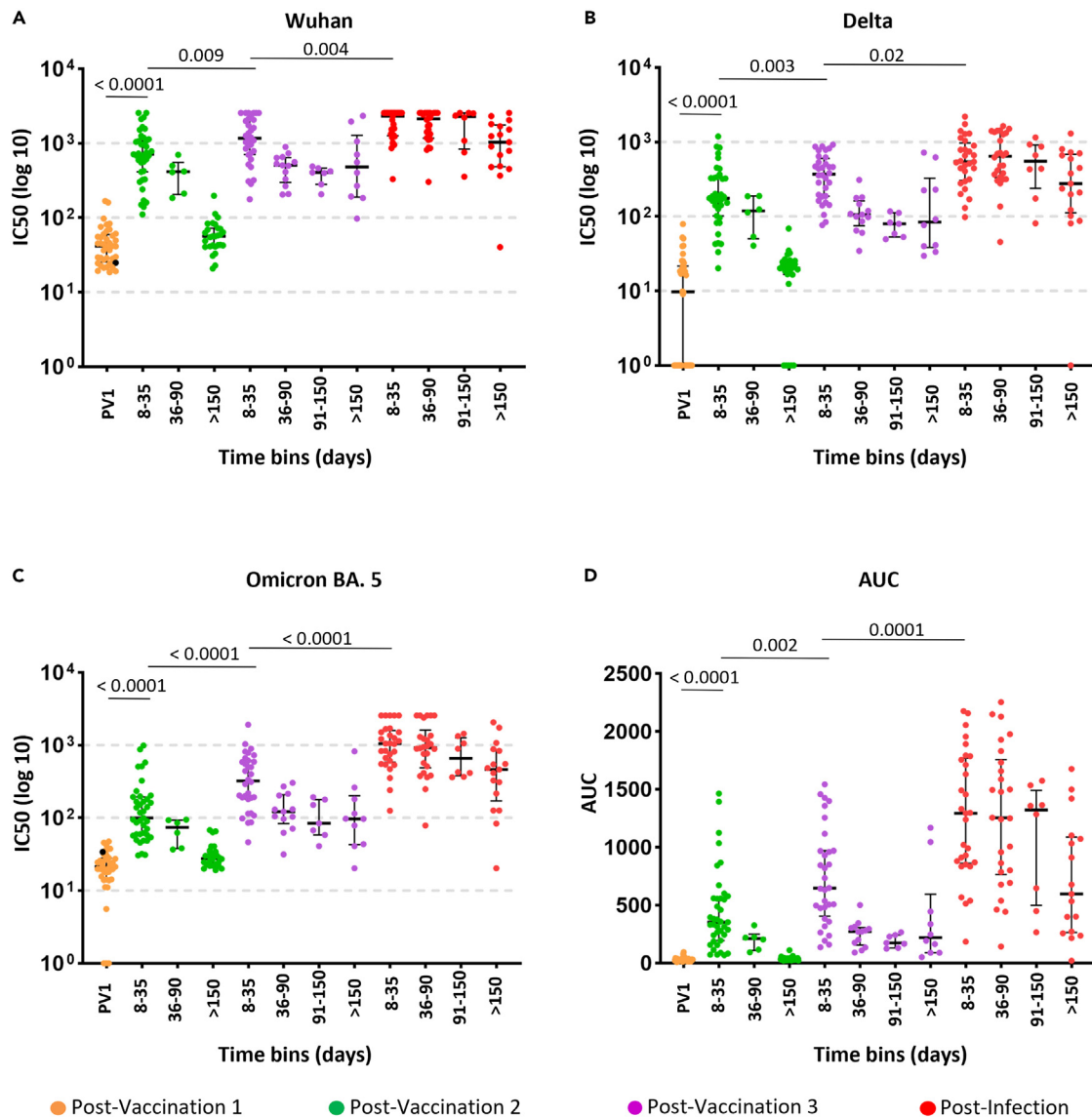
Figure 3. Dynamics of antibody neutralization during vaccination and after breakthrough infection

Neutralization was tested for original Wuhan (A), Delta (B), and Omicron BA.5 (C) strains using a lentiviral pseudovirus neutralization assay at post-vaccination 1 (PV1, orange), post-vaccination 2 (green), post-vaccination 3 (purple), and BTI (red). The area under the curve (AUC) was calculated for the neutralization of the three variants to determine the neutralization breadth for each time point (D). If multiple samples were available within one time frame, the highest IC_{50} value was reported for the peak response at 8–35 days after vaccination or infection. For the other time points, a mean IC_{50} value was calculated if more than one data point was present. The upper limit of detection was an IC_{50} value of 2,560, while the lower cutoff was 20. Statistical analyses were performed using the Mann-Whitney test. Median values, interquartile range, and *p* values below 0.05 are indicated.

associated with persistent high levels of cross-neutralizing antibody responses to spike, as well as broad and persistent T cell reactivity to the non-vaccine-encoded virion antigens N and M.

Vaccine-induced peak neutralizing antibody IC_{50} titers are associated with risk reduction of Omicron variant infection

In order to address whether vaccine-induced antibody and/or S-specific T cell responses at least temporarily protected from SARS-CoV-2 Omicron variant infection; we estimated hazard ratios (HRs) using Cox regression. As covariates in our model, we separated study volunteers into two groups based on levels of antibody IC_{50} values or S-specific $CD4^+$ or $CD8^+$ T cell frequencies at peak response (8–35 days after third vaccination). The cutoff values for each covariate were optimized to separate between "protected" and "non-protected" individuals.

Omicron BA.5 neutralization IC_{50} values above 400 were more significantly associated with a reduced hazard for Omicron infection (HR [95% confidence interval (CI)] = 0.27 [0.1–0.7], *p* = 0.007, Figure 6A), compared to Delta (IC_{50} values above 506, HR [95% CI] = 0.3 [0.11–0.81], *p* = 0.019,
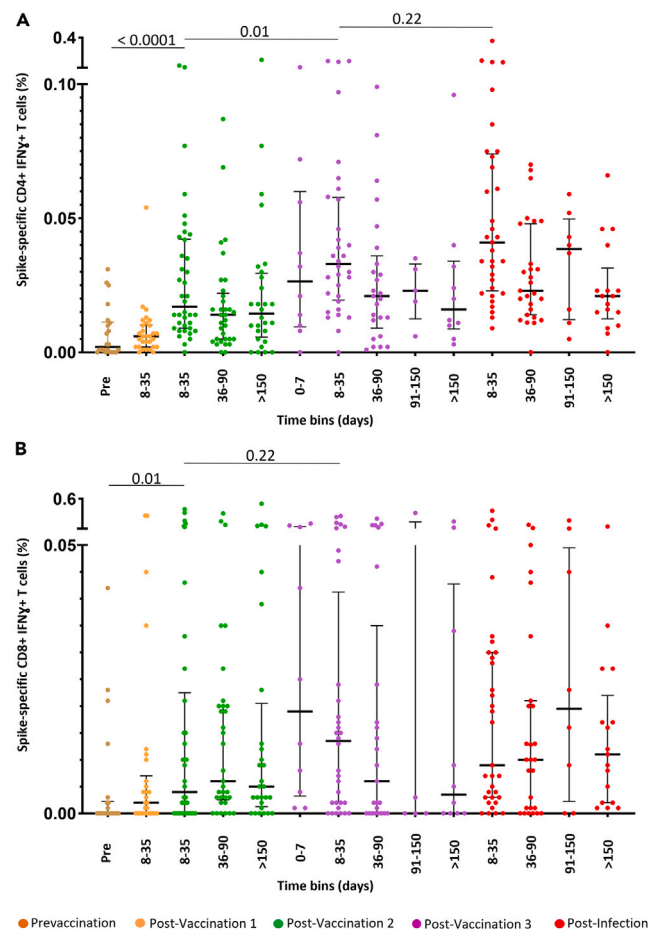
Figure 4. Dynamics of SARS-CoV-2-specific T cell responses against vaccine-encoded spike protein
The frequency of S-specific IFNγ+ CD4$^+$ (A) and CD8$^+$ (B) T cells before vaccination (Pre, brown), post-vaccination 1 (orange), post-vaccination 2 (green), post-vaccination 3 (purple), and after BTI (red). The time bins after each vaccination and BTI are shown on the x axis. The median and interquartile range are shown; whiskers extend up to the last point inside 1.5 × (IQ3–IQ1) range (Tukey definition). The Mann-Whitney test was used for statistical analyses. *p* values below 0.05 are indicated.

Figure 6B) and Wuhan neutralization (IC$_{50}$ values above 1992, HR [95% CI] = 0.4 [0.16–1], *p* = 0.05, Figure 6C). Of note, for many participants and time points, the IC$_{50}$ values for the Wuhan variant were often above the dynamic range of the neutralization assay, which likely affected this HR calculation. Circulating S-specific IFNγ+ CD4$^+$ or CD8$^+$ T cell frequencies were not significantly associated with a change in the infection risk (Figures S5A and S5B). A multivariate Cox regression model considering Omicron BA.5 neutralizing antibody levels, S-specific CD4$^+$ and S-specific CD8$^+$ T cell frequencies, showed a significant risk reduction only for Omicron BA.5 neutralizing antibody levels (HR [95% CI] = 0.3 [0.11–0.8]) (Figure 6D). Together, these results demonstrate that a vaccine-induced cross-neutralizing antibody response was associated with a significant reduction in hazard of Omicron infection when accounting for S-specific CD4$^+$ and S-specific CD8$^+$ T cell responses.

Effect of neutralizing antibodies on the infection risk against Omicron BA.5

We utilized a mathematical model to determine the role of neutralizing antibodies in protection from Omicron infection during the observed time period and protection from future re-infection by an unknown Omicron strain. A schematic representation of the model can be found in Figure 7A. This model describes the infection risk of individuals based on (i) their time-dependent antibody IC$_{50}$ level and (ii) the time-dependent number of infectious individuals in the general population. More precisely, the infection risk is expressed by a hazard rate *h(t)* which is influenced by the IC$_{50}$ neutralizing antibody titers of the individual (Antibodies(t)) at any given time and the seven-day SARS-CoV-2 infection incidence (Incidence(t)) per 100,000 inhabitants in Bavaria (Figure 7A). In this model higher Antibodies(t) reduce infection risk, whereas a higher Incidence(t) increases it. The model contains two parameters: the base risk of infection for the Omicron lineage, β_0, and the estimated effect of antibody levels on infection risk, β_1. Infection risk parameters were chosen based on the literature.[20–23]

The effect of antibody levels on infection risk, β_1, was inferred from the time-to-infection data from individuals as well as the matching antibody levels. Using these parameters (β_0 and β_1), the infection risks for individuals can be studied and visualized. In Figure 7B
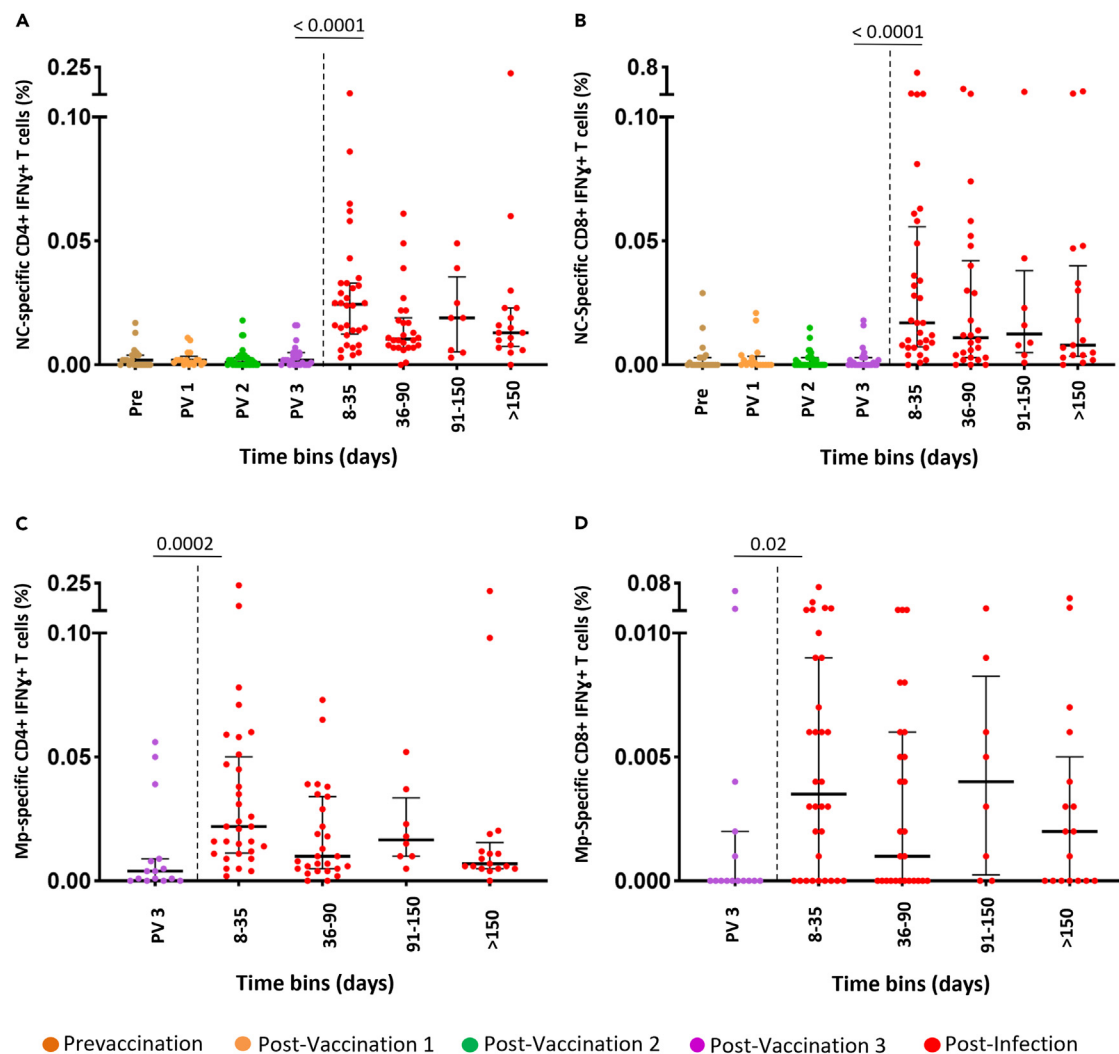
Figure 5. Dynamics of SARS-CoV-2-specific T cell responses against non-vaccine-encoded antigens

The frequency of N-specific IFNγ+ $CD4^+$ (A) and $CD8^+$ (B) and membrane-specific IFNγ+ $CD4^+$ (C) and $CD8^+$ (D) T cells before vaccination (Pre, brown), post-vaccination 1 (PV1, orange), post-vaccination 2 (PV2, green), post-vaccination 3 (PV3, purple), and after BTI (red). The time bins after each vaccination and BTI are shown on the x axis. The median and interquartile range are shown; whiskers extend up to the last point inside 1.5*(IQ3–IQ1) range (Tukey definition). The Mann-Whitney test was used for statistical analyses. p values below 0.05 are indicated.

example trajectories of the seven-day incidence (left panel) and IC_{50} neutralizing antibody titers (right panel) are shown for three representative individuals prior to an infection. Although only a minor variation in the risk of infection was observed between individuals 1 and 3, individual 2 clearly diverges and appears to be protected during the peak incidence in Bavaria between February and May. The higher neutralizing antibody titers observed within individual 2 as compared to individual 1 and 3 potentially contributed to protection (Figure 7B, right panel).

As the base risk of infection for the Omicron lineage, β_0, is not precisely known, we compared different literature estimates of the base risk of infection and our estimated effect β_1 of antibody levels on infection risk (Figure 7C, right panel). Considering BA.5 neutralization data from all 31 BTIs, the effect did not depend strongly on the base infection risk factor β_0, leading to similar infection risk reduction for any given antibody IC_{50} value (Figure S6). The different estimates for β_1 result in a reduction of infection risk that quickly rises with an increase in the neutralizing antibody titers. Antibody levels at the upper detection limit (IC_{50} value of 2,560) reduce the risk of infection by almost 100%.

Finally, after determining the effect of the antibodies on the infection risk within our cohort for triple-vaccinated individuals, we utilized the BA.5 IC_{50} neutralizing antibody titers after BTI (assuming these correlate with neutralization of other Omicron variants[24]) to simulate the risk of a second infection with a SARS-CoV-2 Omicron variant (Figure 7D). In our simulation, the increased neutralizing antibody levels after BTI strongly reduce the infection risk within 180 days compared to three vaccinations. The model predicts several infections within these 180 days, which were however not observed in our study volunteers.
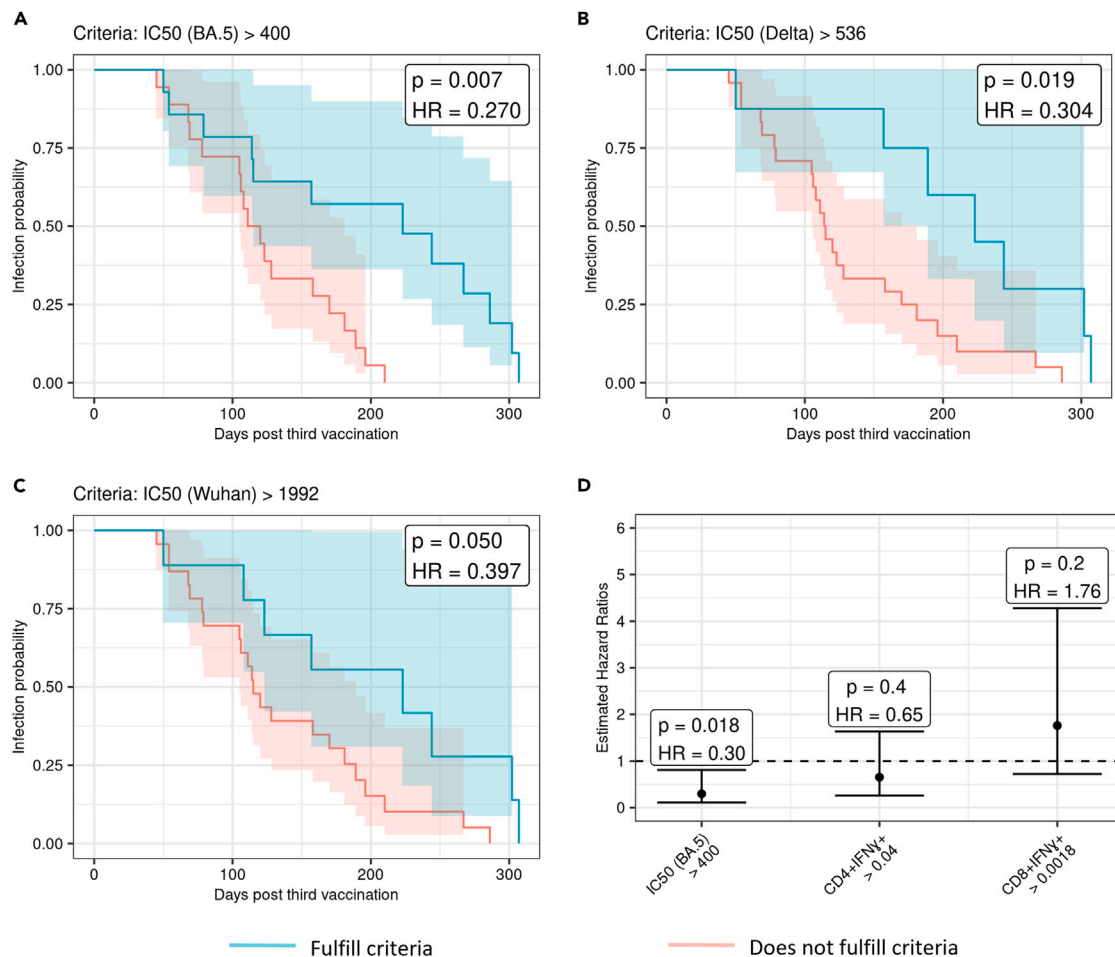
Figure 6. Survival analysis of infections in triple-vaccinated participants in relation to neutralizing antibody

The estimated survival probability after three vaccinations (*n* = 32) depending on the level of antibodies between day 8 and 35 after the vaccination for those above (green) and those below (red) the IC$_{50}$ cutoff are shown for Omicron BA.5 (A), Delta (B), and the original Wuhan strain (C). The respective cutoff criteria are indicated above each graph. Events are BTI and time is measured in days after vaccination. (D) Displays the corresponding hazard ratios and confidence intervals estimated from a Cox regression model.

Modeling the effect of pre-existing nucleocapsid-specific T cells on upper airway viral load upon hypothetical re-infection with a neutralization-resistant SARS-CoV-2 variant

To estimate the effect of circulating SARS-CoV-2-specific T cells on the upper airway viral load (UA-VL) during a hypothetical second infection with a completely neutralization-resistant virus variant, we employed a linear mixed-effects model previously described by Eser et al.[11] A schematic comparison of estimated viral load levels within 7 days after secondary infection between a patient with or without pre-existing memory SARS-CoV-2 N-specific CD4$^+$ T cells is shown in Figure 8A. Using measurements from this study we have modeled the frequency of pre-existing N-specific T after a hypothetical second infection at 180 days after the initial BTI (Figure 8B). Assuming that no expansion of pre-existing N-specific T cells occurred upon second infection (i.e., the fold expansion is equal to one), a reduction of UA-VL between 7.3% and 23.0% is predicted (Figure 8C). As highly variable expansion of pre-existing influenza M- and N-specific T cells was observed during human influenza challenge experiments with an average of 10-fold increase at day seven, we have investigated the impact of it on the results of the model.[25] According to our model, an estimated 10-fold expansion of N-specific CD4$^+$ T cells could reduce acute infection UA-VL by 77.5% (53.0%–92.7%) on average compared to previously non-exposed individuals (Figure 8C). In summary, pre-existing N-specific CD4$^+$ IFNγ+ T cells induced by a first BTI are likely to associate with a multi-fold reduction of acute-phase viral load upon a re-infection compared to first infection.

DISCUSSION

We investigated the evolution of peripheral SARS-CoV-2-specific antibody and T cell responses in a longitudinal Bavarian cohort during vaccination and upon subsequent BTI from February 2021 to December 2022. The study data were then utilized to assess the risk for re-infection as a
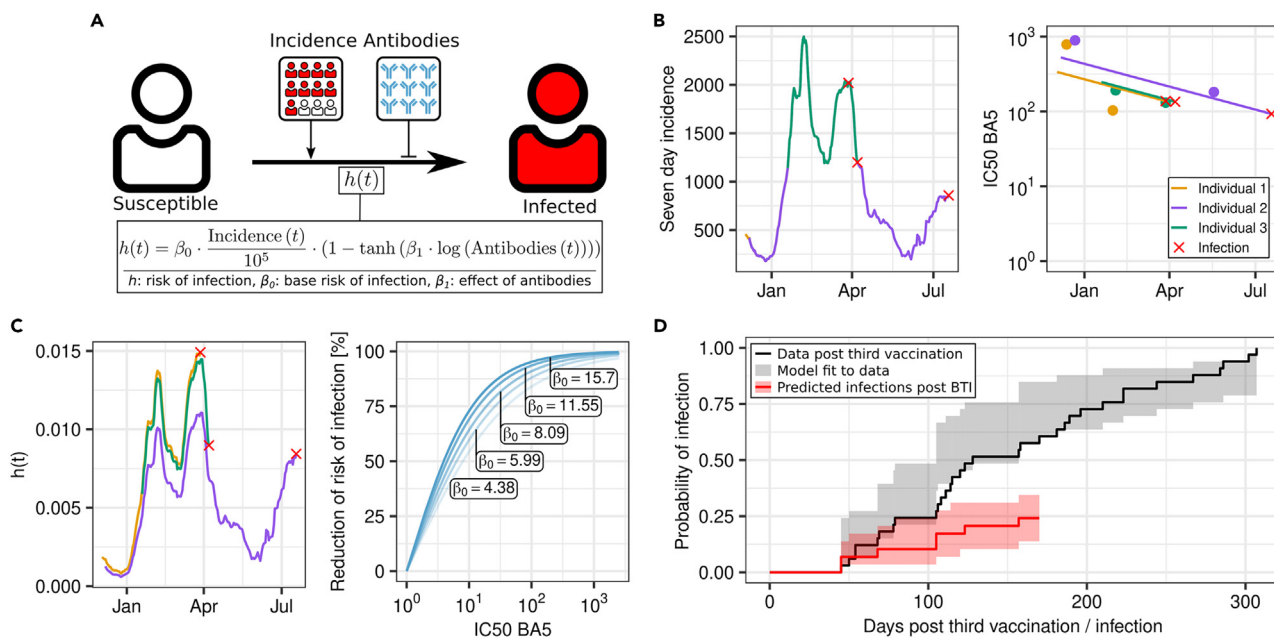
Figure 7. Reduction of infection risk through neutralizing antibodies

A schematic representation of the model with a susceptible person (S) that becomes infected (I) is shown in (A). This model shows the risk of infection ($h(t)$), which is dependent on the seven-day incidence per 100,000 inhabitants in Munich (Incidence(t)) and the neutralizing antibody titers (Antibodies(t)), where a high incidence increases the infection risk ($h(t)$) and vice versa for the antibodies. Different parameter values for the Omicron variant baseline infection risk β_0 were obtained from literature.[20–23] The effect of the antibodies is represented by β_1 and was estimated from the data of this study. The current seven-day incidence in Munich (B, left panel) and IC_{50} neutralizing antibody titers (B, right panel) are shown for three representative individuals after their third vaccination until the time of infection. The antibody level is estimated from a linear mixed-effects model. The hazard rate for the different individuals is shown in (C) (left panel) for $\beta_0 \approx 11.55$ and $\beta_1 \approx 0.36$. Different base infection risk parameters were utilized to present the reduction in the infection risk via the IC_{50} antibody neutralizing titers (C, right panel). In (D), we show the distribution of infections from data of this study (black line), our model fit to the data (gray shaded area), and results of a simulation study in which individuals become infected after their BTI (red). Given our estimate of β_0 and β_1 from (C, left panel), seven-day incidence in Munich and measurements of antibody levels after BTI, samples were drawn from the estimated cumulative distribution function after BTI up to 180 days after infection (limit of reported incidence at time of analysis). The shaded areas indicate the 2.5%–97.5% simulation quantiles. The red solid line indicates the media simulation values.

function of neutralizing antibody titers and—in case of re-infection with a hypothetical, completely neutralization–resistant new variant—to estimate the effect of pre-existing SARS-CoV-2-specific memory T cell responses on the UA-VL. Despite triple vaccination, 97% of the study participants experienced BTI within one year of the last vaccination. Re-infection only occurred in 4 individuals consistent with high protective efficiency against re-infection after Omicron BTI. Peak Omicron BA.5 neutralization IC_{50} titers after the third vaccination were the strongest correlate of transient protection from Omicron infection, while S-specific $CD4^+$ and $CD8^+$ T cell frequencies did not correlate with a reduced infection risk. Surprisingly, 42% of vaccinees with peak BA.5 IC_{50} values above 400 (and likely higher IC_{50}s for BA.1/2) were infected within 120 days after the third vaccination in early 2022.[26] During the early phase 3 vaccine efficiency trials, even peak "Wuhan" IC_{50} values above 100 were associated with a protective efficiency of above 90%.[3,5] Lower protective IC_{50} in our study may be explained by the fact that phase-3-vaccine-trial participants, at that time, encountered a virus strain more homologous to the vaccine. In addition, extraordinarily high numbers of virus encounters during the Omicron BA.1/2 wave likely contributed to these BTIs in the presence of high neutralizing antibody titers. Of note, our mathematical model suggested that Omicron BA.5 IC_{50} titers above 400 reduce the infection risk by more than 90% against Omicron BA.5 infection, which is in the similar range as described for the phase 3 vaccine trials of the pre-Omicron era.[27–31] One possible explanation for the difference in our results compared to the clinical trials could therefore be the high incidence and associated high number of virus encounters in Bavaria in early 2022, which was multifold higher as compared to July 2020 to March 2021, when these trials were conducted. Protection from SARS-CoV-2 Omicron infection in Bavaria in early 2022 therefore likely required higher titers and breadth of neutralizing antibodies as compared to the pre-Omicron era. Some methodological variability such as different amounts of input virus in the neutralization assay may also contribute to these differences in protective titers.

Differences in incident infection dynamics between high and low titer groups became more apparent beyond 4 months after the 3rd vaccination, which, for most participants, coincided with the onset of spring-summer season and a season-associated reduction of infection incidence, until emergence of the more virulent BA.4/5 and its sub-lineages (BQ.1, BF.1, and BQ.1.1) starting from May/June 2022 (data obtained from Bay-VOC).[32]

Omicron BTIs further increased neutralization against the three tested variants significantly. While Wuhan- and Delta-specific neutralization was also enhanced, the strongest effect was observed for Omicron BA.5 neutralization. Furthermore, our magnitude-breadth analysis show significantly increased breadth of neutralization after BTI likely conveying improved protection from re-infection despite the evolution of novel
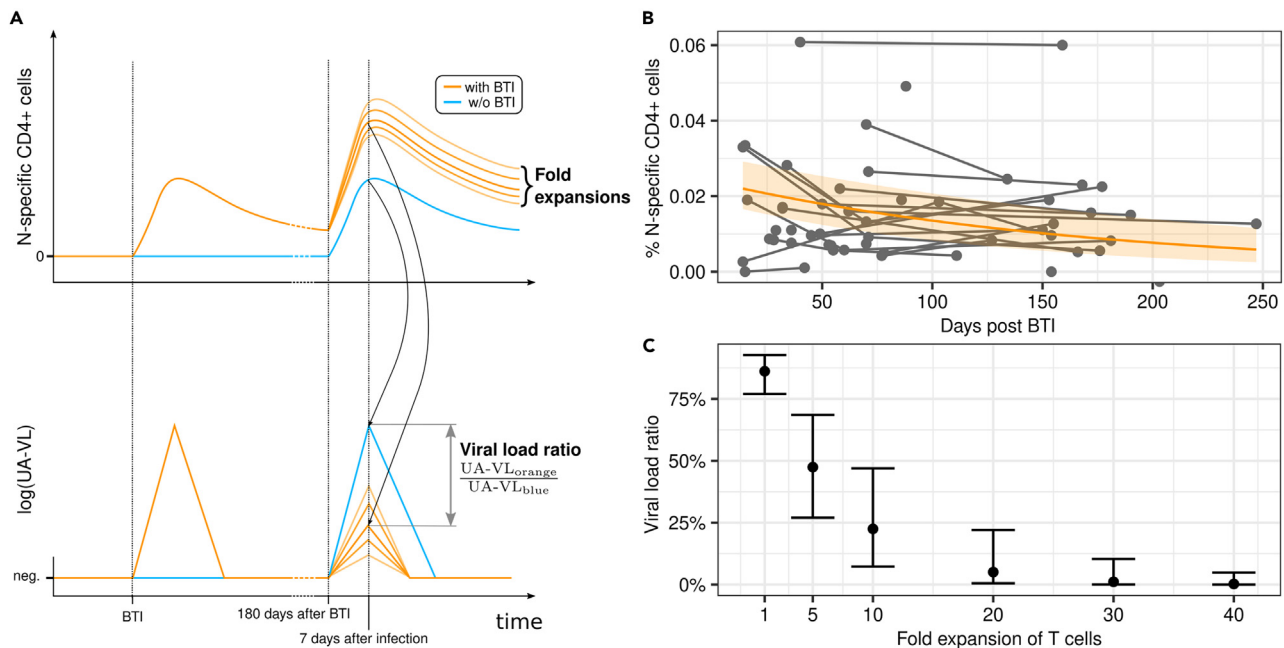
Figure 8. Theoretical reduction of viral load through pre-existing nucleocapsid-specific CD4+IFNγ+ T cells

(A) shows theoretical trajectories of N-specific CD4+IFNγ+ T cells and upper airway viral (UA-VL) load after BTI and after an additional infection at 180 days after BTI. Trajectory of an individual who experienced a BTI (orange) and who has not experienced the BTI (blue); both are subsequently infected at 180 days after BTI time point. Measured nucleocapsid CD4+IFNγ+ T cells after BTI with a fitted exponential decay model are displayed in (B, orange line). The orange-shaded area represents the 95% confidence interval for the estimated fixed effect parameters. Using the level of N-specific CD4+IFNγ+ T cells at 180 days after BTI and different cell expansion factors, we can estimate the approximate T cell level at 7 days after secondary infection and compare it to measurements from individuals without previous infection.[11] The difference (displayed as a ratio) in viral load of individuals with and without pre-existing T cells derived from a linear mixed-effects model based on Eser et al. is shown in (C).

more neutralization-resistant variants. Our mathematical model further supported the concept that high neutralizing antibody titers after Omicron BTI contribute to protection from subsequent re-infection. Interestingly, the protection in our cohort was higher than predicted by our model considering only the antibody levels reached after a BTI, consistent with a protective role of cell-mediated immunity against re-infection.

Even long after BTI, we observed broad memory T cell recognition against the three tested virus antigens S, M, and N, similar to what was observed in non-BTI Wuhan infection,[16,33] and these—according to our model—possibly contributed to the high level of protection observed in our cohort after BTI. Indeed, pre-existing T cells, in particular those targeting the N protein, have been associated with protection from SARS-CoV-2 infection.[14,15,34] Moreover, N-specific T cell responses are also associated with control of SARS-CoV-2 in the upper airways and reduced systemic inflammation.[11] The effect of pre-existing T cells on virus control and early T cell expansion was studied after controlled influenza challenge of human volunteers.[25] Key results from the Eser and Wilkinson studies[11,25] were therefore utilized to estimate the effect of pre-existing SARS-CoV-2-specific memory T cells on UA-VL upon a hypothetical re-infection with a neutralization-resistant SARS-CoV-2 variant. Assuming that the T cell expansion during SARS-CoV-2 behaves similar to influenza and the effect of T cells on virus clearance is unchanged between the first and second infection, individuals with circulating SARS-CoV-2-specific T cells, in particular those targeting N, likely control the neutralization-resistant virus efficiently. This process may depend on the level of pre-existing virus-specific memory T cells and should reduce onward transmission and may even abort infection early.[14,15,35] Both primary and BT infection also result in the formation of airway tissue-resident memory T cells, which differs from intramuscular vaccination.[17,19] BTI can therefore be considered as airway immunization. It should be noted that vaccination-induced formation of T cell memory in the airway tissues is a key determinant for infection outcome in small rodent and non-human primate studies.[12,13,36,37] One recent clinical study showed that, after BTI, SARS-CoV-2-specific tissue-resident memory T cells persist in the upper airways at similar levels up to 3 months but by month 6 have declined.[17] This decay of mucosal adaptive immunity and the recruitment dynamics of virus-specific tissue-resident T cells into the airways upon re-exposure likely influence the outcome upon virus re-exposure and need to be investigated in future studies.

The presented study had several limitations. We did not test neutralization with the autologous infecting virus variant, as most participants were infected during the Omicron BA.1/2 wave. Moreover, T cell responses were only tested against three immunodominant antigens in blood and not tested within the airway tissues. Furthermore, the mathematical models used for data analysis provided only a simplified description of real-world processes. The model for the assessment of the infection risk makes, for instance, use of information on the time-varying risk of infection (based on incidence) with a high-time resolution but constructs estimate for each individuals' antibody trajectory from observations with low-time resolution, which introduces some uncertainty. However, by simulating infections of several individuals from

our model, we were able to confirm that the model accurately describes the data presented herein. Further, an accurate account of the exact number of infected people in Bavaria is difficult to obtain, due to reporting issues, and only the official numbers reported by the RKI were used in this study. Nevertheless, the infection process in this study could be reliably recapitulated using our model. Thus, we believe the model provides valuable insights into the risk reduction through neutralizing antibodies against SARS-CoV-2.

In conclusion, this study revealed that Omicron BTI induced a state of hybrid immunity characterized by higher cross-reactive, more persistent neutralizing antibody responses and broader SARS-CoV-2-specific T cell responses. These characteristics aligned with a high level of protection from re-infection and—in the case of re-infection—reduced UA-VLs as suggested by our model. Events on a population scale likely reflect induction of protective immunity upon BTI in Bavaria; Omicron waves occurred until October 2022 in the Bavarian population but waned thereafter despite the onset of the winter season. These data therefore suggest that BTI-induced hybrid immunity was an important contributor to the reduced virus transmission observed in the early winter of 2022. Future studies therefore should address whether intramuscular followed by intranasal immunization with attenuated respiratory viruses can induce broadly cross-protective hybrid immunity and assess its durability.

CONSORTIA

ORCHESTRA/KoCo19 working group: Mohamed Ibraheem Mohamed Ahmed, Emad Alamoudi, Jared Anderson, Maximilian Baumann, Marc Becker, Marieke Behlen, Jessica Beyerl, Rebecca Böhnlein, Isabel Brand, Anna Brauer, Vera Britz, Jan Bruger, Friedrich Caroli, Lorenzo Contento, Max Diefenbach, Jana Diekmannshemke, Paulina Diepers, Anna Do, Gerhard Dobler, Jürgen Durner, Ute Eberle, Judith Eckstein, Tabea Eser, Volker Fingerle, Jonathan Frese, Felix Förster, Turid Frahnow, Günter Fröschl, Christiane Fuchs, Mercè Garí, Otto Geisenberger, Leonard Gilberg, Kristina Gillig, Philipp Girl, Arlett Heiber, Christian Hinske, Janna Hoefflin, Tim Hofberger, Michael Höfinger, Larissa Hofmann, Sacha Horn, Kristina Huber, Christian Janke, Ursula Kappl, Charlotte Kiani, Arne Kroidl, Michael Laxy, Ronan Le Gleut, Reiner Leidl, Felix Lindner, Silke Martin, Rebecca Mayrhofer, Anna-Maria Mekota, Hannah Müller, Katharina Müller, Dafni Metaxa, Leonie Pattard, Michel Pletschette, Michael Pritsch, Stephan Prückner, Konstantin Pusl, Peter Pütz, Ernst-Markus Quenzel, Katja Radon, Elba Raimúndez, Camila Rothe, Nicole Schäfer, Yannik Schälte, Paul Schandelmaier, Lara Schneider, Sophie Schultz, Mirjam Schunk, Lars Schwettmann, Heidi Seibold, Peter Sothmann, Paul Stapor, Fabian Theis, Verena Thiel, Sophie Thiesbrummel, Niklas Thur, Julia Waibel, Claudia Wallrauch, Franz Weinauer, Simon Winter, Julia Wolff, Pia Wullinger, Houda Yaqine, Sabine Zange, Eleftheria Zeggini, Thomas Zimmermann, Anna Zielke.

STAR★METHODS

Detailed methods are provided in the online version of this paper and include the following:

- KEY RESOURCES TABLE
- RESOURCE AVAILABILITY
  - ○ Lead contact
  - ○ Materials availability
  - ○ Data and code availability
- EXPERIMENTAL MODEL AND STUDY PARTICIPANT DETAILS
- METHOD DETAILS
  - ○ Assessment of SARS-CoV-2 strains
  - ○ Pseudovirus neutralization assay
  - ○ Binding antibody titers
  - ○ Flow cytometry
- QUANTIFICATION AND STATISTICAL ANALYSIS
  - ○ Statistical modelling
  - ○ Infection model
  - ○ Reduction in viral load by pre-existing nucleocapsid specific T cells

SUPPLEMENTAL INFORMATION

Supplemental information can be found online at https://doi.org/10.1016/j.isci.2024.110138.

AUTHOR CONTRIBUTIONS

DECLARATION OF INTERESTS

REFERENCES

1. Flechsler, J., Eberle, U., Dangel, A., Hepner, S., Wimmer, C., Lutmayr, J., Konrad, R., Berger, C., Weise, L., Sprenger, A., et al. (2022). Molecular SARS-CoV-2 surveillance in Bavaria shows no Omicron transmission before the end of November 2021. Infection 50, 761–766. https://doi.org/10.1007/s15010-022-01767-1.

2. Taylor, L. (2022). Covid-19: Omicron drives weekly record high in global infections. BMJ 376, o66. https://doi.org/10.1136/bmj.o66.

3. Maier, B.F., Wiedermann, M., Burdinski, A., Klamser, P.P., Jenny, M.A., Betsch, C., and Brockmann, D. (2022). Germany's fourth COVID-19 wave was mainly driven by the unvaccinated. Commun. Med. 2, 116. https://doi.org/10.1038/s43856-022-00176-7.

4. (2022). Varianten bei COVID-19 Patienten in Bayern. https://www.bay-voc.lmu.de/surveillance.xhtml.

5. Petrone, D., Mateo-Urdiales, A., Sacco, C., Riccardo, F., Bella, A., Ambrosio, L., Lo Presti, A., Di Martino, A., Ceccarelli, E., Del Manso, M., et al. (2023). Reduction of the risk of severe COVID-19 due to Omicron compared to Delta variant in Italy (November 2021 - February 2022). Int. J. Infect. Dis. 129, 135–141. https://doi.org/10.1016/j.ijid.2023.01.027.

6. Bayerisches Landesamt für Gesundheit und Lebensmittelsicherheit (2021). Coronavirus-Infektionszahlen in Bayern. https://www.lgl.bayern.de/gesundheit/infektionsschutz/infektionskrankheiten_a_z/coronavirus/karte_coronavirus/index.htm.

7. Gilbert, P.B., Montefiori, D.C., McDermott, A.B., Fong, Y., Benkeser, D., Deng, W., Zhou, H., Houchens, C.R., Martins, K., Jayashankar, L., et al. (2022). Immune correlates analysis of the mRNA-1273 COVID-19 vaccine efficacy clinical trial. Science 375, 43–50. https://doi.org/10.1126/science.abm3425.

8. Feng, S., Phillips, D.J., White, T., Sayal, H., Aley, P.K., Bibi, S., Dold, C., Fuskova, M., Gilbert, S.C., Hirsch, I., et al. (2021). Correlates of protection against symptomatic and asymptomatic SARS-CoV-2 infection. Nat. Med. 27, 2032–2040. https://doi.org/10.1038/s41591-021-01540-1.

9. Corbett, K.S., Nason, M.C., Flach, B., Gagne, M., O'Connell, S., Johnston, T.S., Shah, S.N., Edara, V.V., Floyd, K., Lai, L., et al. (2021). Immune correlates of protection by mRNA-1273 vaccine against SARS-CoV-2 in nonhuman primates. Science 373, eabj0299. https://doi.org/10.1126/science.abj0299.

10. Mercado, N.B., Zahn, R., Wegmann, F., Loos, C., Chandrashekar, A., Yu, J., Liu, J., Peter, L., McMahan, K., Tostanoski, L.H., et al. (2020). Single-shot Ad26 vaccine protects against SARS-CoV-2 in rhesus macaques. Nature 586, 583–588. https://doi.org/10.1038/s41586-020-2607-z.

11. Eser, T.M., Baranov, O., Huth, M., Ahmed, M.I.M., Deák, F., Held, K., Lin, L., Pekayvaz, K., Leunig, A., Nicolai, L., et al. (2023). Nucleocapsid-specific T cell responses associate with control of SARS-CoV-2 in the upper airways before seroconversion. Nat. Commun. 14, 2952. https://doi.org/10.1038/s41467-023-38020-8.

12. Zhao, J., Zhao, J., Mangalam, A.K., Channappanavar, R., Fett, C., Meyerholz, D.K., Agnihothram, S., Baric, R.S., David, C.S., and Perlman, S. (2016). Airway Memory CD4(+) T Cells Mediate Protective Immunity against Emerging Respiratory Coronaviruses. Immunity 44, 1379–1391. https://doi.org/10.1016/j.immuni.2016.05.006.

13. Ishii, H., Nomura, T., Yamamoto, H., Nishizawa, M., Thu Hau, T.T., Harada, S., Seki, S., Nakamura-Hoshi, M., Okazaki, M., Daigen, S., et al. (2022). Neutralizing-antibody-independent SARS-CoV-2 control correlated with intranasal-vaccine-induced CD8(+) T cell responses. Cell Rep. Med. 3, 100520. https://doi.org/10.1016/j.xcrm.2022.100520.

14. Swadling, L., Diniz, M.O., Schmidt, N.M., Amin, O.E., Chandran, A., Shaw, E., Pade, C., Gibbons, J.M., Le Bert, N., Tan, A.T., et al. (2022). Pre-existing polymerase-specific T cells expand in abortive seronegative SARS-CoV-2. Nature 601, 110–117. https://doi.org/10.1038/s41586-021-04186-8.

15. Kundu, R., Narean, J.S., Wang, L., Fenn, J., Pillay, T., Fernandez, N.D., Conibear, E., Koycheva, A., Davies, M., Tolosa-Wright, M., et al. (2022). Cross-reactive memory T cells associate with protection against SARS-CoV-2 infection in COVID-19 contacts. Nat. Commun. 13, 80. https://doi.org/10.1038/s41467-021-27674-x.

16. Wyllie, D., Jones, H.E., Mulchandani, R., Trickey, A., Taylor-Phillips, S., Brooks, T., Charlett, A., Ades, A., Moore, P., Boyes, J., et al. (2021). SARS-CoV-2 responsive T cell numbers and anti-Spike IgG levels are both associated with protection from COVID-19: A prospective cohort study in keyworkers. Preprint at medRxiv. https://doi.org/10.1101/2020.11.02.20222778.

17. Lim, J.M.E., Tan, A.T., Le Bert, N., Hang, S.K., Low, J.G.H., and Bertoletti, A. (2022). SARS-CoV-2 breakthrough infection in vaccinees induces virus-specific nasal-resident CD8+ and CD4+ T cells of broad specificity. J. Exp. Med. 219, e20220780. https://doi.org/10.1084/jem.20220780.

18. Ahmed, M.I.M., Diepers, P., Janke, C., Plank, M., Eser, T.M., Rubio-Acero, R., Fuchs, A., Baranov, O., Castelletti, N., Kroidl, I., et al. (2022). Enhanced Spike-specific, but attenuated Nucleocapsid-specific T cell responses upon SARS-CoV-2 breakthrough versus non-breakthrough infections. Front. Immunol. 13, 1026473. https://doi.org/10.3389/fimmu.2022.1026473.

19. Poon, M.M.L., Rybkina, K., Kato, Y., Kubota, M., Matsumoto, R., Bloom, N.I., Zhang, Z., Hastie, K.M., Grifoni, A., Weiskopf, D., et al. (2021). SARS-CoV-2 infection generates tissue-localized immunological memory in humans. Sci. Immunol. 6, eabl9105. https://doi.org/10.1126/sciimmunol.abl9105.

20. Volz, E., Mishra, S., Chand, M., Barrett, J.C., Johnson, R., Geidelberg, L., Hinsley, W.R., Laydon, D.J., Dabrera, G., O'Toole, Á., et al. (2021). Assessing transmissibility of SARS-CoV-2 lineage B.1.1.7 in England. Nature 593, 266–269. https://doi.org/10.1038/s41586-021-03470-x.

21. Ito, K., Piantham, C., and Nishiura, H. (2022). Relative instantaneous reproduction number of Omicron SARS-CoV-2 variant with respect to the Delta variant in Denmark. J. Med. Virol. 94, 2265–2268. https://doi.org/10.1002/jmv.27560.

22. Dandekar, R., and Barbastathis, G. (2020). Neural Network Aided Quarantine Control Model Estimation of Global Covid-19 Spread.

23. (2021). SPI-M-O: Consensus Statement on COVID-19. https://www.gov.uk/government/publications/spi-m-o-consensus-statement-on-covid-19-3-june-2021.

24. Tran, T.T., Vaage, E.B., Mehta, A., Chopra, A., Tietze, L., Kolderup, A., Anthi, A., König, M., Nygaard, G., Lind, A., et al. (2022). Titers of antibodies against ancestral SARS-CoV-2 correlate with levels of neutralizing antibodies to multiple variants. NPJ Vaccines 7, 174. https://doi.org/10.1038/s41541-022-00586-7.

25. Wilkinson, T.M., Li, C.K.F., Chui, C.S.C., Huang, A.K.Y., Perkins, M., Liebner, J.C., Lambkin-Williams, R., Gilbert, A., Oxford, J., Nicholas, B., et al. (2012). Preexisting influenza-specific CD4+ T cells correlate with disease protection against influenza challenge in humans. Nat. Med. 18, 274–280. https://doi.org/10.1038/nm.2612.

26. Cheng, S.S., Mok, C.K., Li, J.K., Ng, S.S., Lam, B.H., Jeevan, T., Kandeil, A., Pekosz, A., Chan, K.C., Tsang, L.C., et al. (2022). Plaque-neutralizing antibody to BA.2.12.1, BA.4 and BA.5 in individuals with three doses of BioNTech or CoronaVac vaccines, natural infection and breakthrough infection. J. Clin. Virol. 156, 105273. https://doi.org/10.1016/j.jcv.2022.105273.

27. Polack, F.P., Thomas, S.J., Kitchin, N., Absalon, J., Gurtman, A., Lockhart, S., Perez, J.L., Pérez Marc, G., Moreira, E.D., Zerbini, C., et al. (2020). Safety and Efficacy of the BNT162b2 mRNA Covid-19 Vaccine. N. Engl. J. Med. 383, 2603–2615. https://doi.org/10.1056/NEJMoa2034577.

28. Baden, L.R., El Sahly, H.M., Essink, B., Kotloff, K., Frey, S., Novak, R., Diemert, D., Spector, S.A., Rouphael, N., Creech, C.B., et al. (2021). Efficacy and Safety of the mRNA-1273 SARS-CoV-2 Vaccine. N. Engl. J. Med. 384, 403–416. https://doi.org/10.1056/NEJMoa2035389.

29. Falsey, A.R., Sobieszczyk, M.E., Hirsch, I., Sproule, S., Robb, M.L., Corey, L., Neuzil, K.M., Hahn, W., Hunt, J., Mulligan, M.J., et al. (2021). Phase 3 Safety and Efficacy of AZD1222 (ChAdOx1 nCoV-19) Covid-19 Vaccine. N. Engl. J. Med. 385, 2348–2360. https://doi.org/10.1056/NEJMoa2105290.

30. Sadoff, J., Gray, G., Vandebosch, A., Cárdenas, V., Shukarev, G., Grinsztejn, B., Goepfert, P.A., Truyers, C., Fennema, H., Spiessens, B., et al. (2021). Safety and Efficacy of Single-Dose Ad26.COV2.S Vaccine against Covid-19. N. Engl. J. Med. 384, 2187–2201. https://doi.org/10.1056/NEJMoa2101544.

31. Logunov, D.Y., Dolzhikova, I.V., Shcheblyakov, D.V., Tukhvatulin, A.I., Zubkova, O.V., Dzharullaeva, A.S., Kovyrshina, A.V., Lubenets, N.L., Grousova, D.M., Erokhova, A.S., et al. (2021). Safety and efficacy of an rAd26 and rAd5 vector-based heterologous prime-boost COVID-19 vaccine: an interim analysis of a randomised controlled phase 3 trial in Russia. Lancet 397, 671–681. https://doi.org/10.1016/S0140-6736(21)00234-8.

32. Kimura, I., Yamasoba, D., Tamura, T., Nao, N., Suzuki, T., Oda, Y., Mitoma, S., Ito, J., Nasser, H., Zahradnik, J., et al. (2022). Virological characteristics of the SARS-CoV-2 Omicron BA.2 subvariants, including BA.4 and BA.5. Cell 185, 3992–4007.e16. https://doi.org/10.1016/j.cell.2022.09.018.

33. Cantoni, D., Mayora-Neto, M., Nadesalingam, A., Wells, D.A., Carnell, G.W., Ohlendorf, L., Ferrari, M., Palmer, P., Chan, A.C.Y., Smith, P., et al. (2022). Neutralisation Hierarchy of SARS-CoV-2 Variants of Concern Using Standardised, Quantitative Neutralisation Assays Reveals a Correlation With Disease Severity; Towards Deciphering Protective Antibody Thresholds. Front. Immunol. 13, 773982. https://doi.org/10.3389/fimmu.2022.773982.

34. Jay, C., Ratcliff, J., Turtle, L., Goulder, P., and Klenerman, P. (2023). Exposed seronegative: Cellular immune responses to SARS-CoV-2 in the absence of seroconversion. Front. Immunol. 14, 1092910. https://doi.org/10.3389/fimmu.2023.1092910.

35. Uddback, I., Michalets, S.E., Saha, A., Mattingly, C., Kost, K.N., Williams, M.E., Lawrence, L.A., Hicks, S.L., Lowen, A.C., Ahmed, H., et al. (2024). Prevention of respiratory virus transmission by resident memory CD8(+) T cells. Nature 626, 392–400. https://doi.org/10.1038/s41586-023-06937-1.

36. Teijaro, J.R., Verhoeven, D., Page, C.A., Turner, D., and Farber, D.L. (2010). Memory CD4 T cells direct protective responses to influenza virus in the lungs through helper-independent mechanisms. J. Virol. 84, 9217–9226. https://doi.org/10.1128/JVI.01069-10.

37. Manfredi, F., Chiozzini, C., Ferrantelli, F., Leone, P., Pugliese, K., Spada, M., Virgilio, A.D., Giovannelli, A., Valeri, M., Cara, A., et al. (2023). Induction of SARS-CoV-2 N-specific CD8+ T cell immunity in lungs by engineered extracellular vesicles associates with strongly impaired viral replication. Preprint at bioRxiv. https://doi.org/10.1101/2023.01.19.524762.

38. Sampson, A.T., Heeney, J., Cantoni, D., Ferrari, M., Sans, M., George, C., Di Genova, C., Mayora Neto, M., Einhauser, S., Asbach, B., et al. (2021). Coronavirus Pseudotypes for All Circulating Human Coronaviruses for Quantification of Cross-Neutralizing Antibody Responses. Viruses 13, 1579. https://doi.org/10.3390/v13081579.

39. Huang, Y., Gilbert, P.B., Montefiori, D.C., and Self, S.G. (2009). Simultaneous Evaluation of the Magnitude and Breadth of a Left and Right Censored Multivariate Response, with Application to HIV Vaccine Development. Stat. Biopharm. Res. 1, 81–91. https://doi.org/10.1198/sbr.2009.0008.

40. Ahmed, M.I.M., Einhauser, S., Peiter, C., Senninger, A., Baranov, O., Eser, T.M., Huth, M., Olbrich, L., Castelletti, N., Rubio-Acero, R., et al. (2023). Evolution of protective SARS-CoV-2-specific B- and T-cell responses upon vaccination and omicron breakthrough infection.

41. Nelder, J.A., and Mead, R. (1965). A simplex method for function minimization. Comput. J. 7, 308–313.

42. Johnson, S.G. (2014). The NLopt nonlinear-optimization package.

43. Cox, D.R. (1972). Regression models and life-tables. J. Roy. Stat. Soc. B Methodol. 34, 187–202. https://doi.org/10.1111/j.2517-6161.1972.tb00899.x.

44. Therneau, T.M., and Grambsch, P.M. (2000). Modeling Survival Data: Extending the Cox Model (Springer).

45. Bartlett, M.S. (1937). Properties of sufficiency and statistical tests. Proc. R. Soc. Lond. A 160, 268–282. https://doi.org/10.1098/rspa.1937.0109.

46. Bates, D., Mächler, M., Bolker, B., and Walker, S. (2015). Fitting Linear Mixed-Effects Models Using lme4. J. Stat. Software 67, 1–48. https://doi.org/10.18637/jss.v067.i01.

47. Lindstrom, M.L., and Bates, D.M. (1990). Nonlinear mixed effects models for repeated measures data. Biometrics 46, 673–687. https://doi.org/10.2307/2532087.

48. Pinheiro, J.C., and Bates, D.M. (2000). Mixed-Effects Models in S and S-PLUS (Springer). https://doi.org/10.1007/b98882.

49. Pinheiro, J., and Bates, D.; R Core Team (2023). nlme: Linear and Nonlinear Mixed Effects Models. R package version 3.1-162.

50. Radon, K., Bakuli, A., Pütz, P., Le Gleut, R., Guggenbuehl Noller, J.M., Olbrich, L., Saathoff, E., Garí, M., Schälte, Y., Frahnow, T., et al. (2021). From first to second wave: follow-up of the prospective COVID-19 cohort (KoCo19) in Munich (Germany). BMC Infect. Dis. 21, 925. https://doi.org/10.1186/s12879-021-06589-4.

51. Eser, T., Baranov, O., Huth, M., Ahmed, M., Deák, F., Held, K., Lin, L., Perkayvaz, K., Leuning, A., Nicolai, L., et al. (2023). Early nucleocapsid-specific T cell responses associate with control of SARS-CoV-2 in the upper airways and reduced systemic inflammation before seroconversion. Nat. Commun. 14, 2952. https://doi.org/10.1038/s41467-023-38020-8.

52. Pritsch, M., Radon, K., Bakuli, A., Le Gleut, R., Olbrich, L., Guggenbühl Noller, J.M., Saathoff, E., Castelletti, N., Garí, M., Pütz, P., et al. (2021). Prevalence and Risk Factors of Infection in the Representative COVID-19 Cohort Munich. Int. J. Environ. Res. Public Health 18, 3572. https://doi.org/10.3390/ijerph18073572.

53. Therneau, T., and Lumley, T. (2015). Package Survival: A Package for Survival Analysis in R. R Package. version 3.5-3.

54. Sjoberg, D., Whiting, K., Curry, M., Lavery, J., and Larmarange, J. (2021). Reproducible Summary Tables with the gtsummary Package. R J. 13, 570–580.

55. Bezanson, J., Edelman, A., Karpinski, S., and Shah, V.B. (2017). Julia: A Fresh Approach to Numerical Computing. SIAM Rev. 59, 65–98. https://doi.org/10.1137/141000671.

56. Pinheiro, J., Bates, D., DebRoy, S., Sarkar, D., and Team, R.C. (2018). nlme: Linear and Nonlinear Mixed Effects Models. R Package Version 3.1-137.

STAR★METHODS

KEY RESOURCES TABLE

REAGENT or RESOURCE	SOURCE	IDENTIFIER
Antibodies		
BD™ Purified Mouse Anti-Human CD28	BD Biosciences	Cat#340975; RRID:AB_400197
BD™ Purified Mouse Anti-Human CD49d	BD Biosciences	Cat#340976; RRID:AB_400198
CD4-ECD, clone: SFCI12T4D11	Beckman Coulter	Cat#6604727; RRID:AB_2833032
CD8-APC-A750, clone: B9.11	Beckman Coulter	Cat#A94686; RRID:2313773
CD3-APC-A700, clone: UCHT1	Beckman Coulter	Cat#B10823; RRID:2313773
FITC anti-human IFN-γ Antibody, clone: B27	Biolegend	Cat#506504; RRID:AB_315437
PE anti-human IL-2 Antibody, clone: MQ1-17H12	Biolegend	Cat#500307; RRID:AB_315094
Brilliant Violet 510™ anti-human TNF-α Antibody	Biolegend	Cat#502950; RRID:AB_2565860
Chemicals, peptides, and recombinant proteins		
Brefeldin A aus *Penicillium* brefeldianum	Sigma Aldrich	Cat#B7651-5MG
Staphylococcal enterotoxin B from *Staphylococcus aureus*	Sigma Aldrich	Cat#S4881-1MG
eBioscience™ Foxp3/Transcription Factor Staining Buffer	eBioscience™	Cat#00-5523-00
PepTivator® SARS-CoV-2 Prot_S1	Miltenyi Biotec	Cat#130-127-041
PepTivator® SARS-CoV-2 Prot_N	Miltenyi Biotec	Cat#130-126-699
PepTivator® SARS-CoV-2 Prot_M	Miltenyi Biotec	Cat#130-126-702
Puromycin for cultivation of HEK293T-ACE2	InvivoGen	Cat#ant-pr-1
Critical commercial assays		
Bright Glo Luciferase Assay System	Promega	Cat#E2650
Experimental models: Cell lines		
HEK-293T	ATCC	Cat#CRL-3216TM
HEK-293T-ACE2 cells	Kindly provided by Prof. Dr. Stefan Pöhlmann, DPZ	
Recombinant DNA		
p8.91	Sampson et al.[38]	https://doi.org/10.3390/v13081579
pCSFLW	Sampson et al.[38]	https://doi.org/10.3390/v13081579
Plasmids with Spike (Alpha, Delta, BA5)	Inserts synthesized at GeneArt	
Software and algorithms		
GraphPad Software version 8	Boston, Massachusetts USA	www.graphpad.com
Python, Python Language Reference, version 3.10.6	Python Software Foundation	https://www.python.org
Python 3.10.12	Ubuntu 'apt'	https://www.python.org/about/
Python package: seaborn 0.12.2	Python 'pip'	https://seaborn.pydata.org/
Python package: pandas 1.5.3	Python 'pip'	https://seaborn.pydata.org/
Python package: numpy 1.26.2	Python 'pip'	https://numpy.org/
Magnitude Breadth Algorithm	Huang et al.[39]	https://doi.org/10.1198/sbr.2009.0008
R version 4.1.2	R Foundation for Statistical Computing, Vienna, Austria	https://www.R-project.org/
Zenodo record for the code used in this publication	Ahmed et al.[40]	https://doi.org/10.5281/zenodo.10814475
Julia version 1.7.2	The Julia Project	https://julialang.org
Nealder mead from Julia package NLopt version 0.6.5	Nelder and Mead[41] Johnson[42]	https://github.com/JuliaOpt/NLopt.jl

Continued

REAGENT or RESOURCE	SOURCE	IDENTIFIER
Cox proportional hazards regression model from the R package survival version 3.5-5	Cox[43] Therneau and Grambsch[44]	https://cran.r-project.org/web/packages/survival
Linear mixed-effects model with restricted maximum likelihood (REML) estimation from the R package lme4 version 1.1-33	Bartlett[45] Bates et al.[46]	https://cran.r-project.org/web/packages/lme4/index.html
Nonlinear mixed-effects model with maximum likelihood estimation from the R package nlme version 3.1-162	Lindstrom and Bates[47] Pinheiro and Bates[48] Pinheiro et al.[49]	https://cran.r-project.org/package=nlme

RESOURCE AVAILABILITY

Lead contact

Any additional information and requests for resources and reagents should be directed to and will be fulfilled by the lead contact, Dr. Christof Geldmacher (geldmacher@lrz.uni-muenchen.de).

Materials availability

This study did not generate new unique reagents.

Data and code availability

- Data have been deposited at Zenodo and are publicly available as of the date of publication. Accession numbers are listed in the key resources table.
- All original code has been deposited at Zenodo and is publicly available as of the date of publication. DOIs are listed in the key resources table.
- Any additional information required to reanalyze the data reported in this paper is available from the lead contact upon request.
- All code is available on Zenodo using the link, https://doi.org/10.5281/zenodo.10814474.

EXPERIMENTAL MODEL AND STUDY PARTICIPANT DETAILS

A total of 50 participants – residing in Bavaria – were recruited into this study between February 2021 and February 2022 as a sub-study of the KoCo19 Study[50] named KoCo19-Immu which allows for longitudinal monitoring of immune responses to SARS-CoV-2.[51] 41 of these were recruited before or shortly after receiving their first SARS-CoV-2 vaccination during the vaccination campaign in the first half of 2021, while additional 9 volunteers were recruited at later time points. All subjects were regularly tested serologically for antibodies against the nucleocapsid protein to confirm of SARS-CoV-2 status throughout the study to detect asymptomatic SARS-CoV-2 infections. Subjects were then followed longitudinally for up to 18 months until December 2022. Whole blood and plasma samples were collected during multiple visits before and after first, second and third vaccinations and after symptomatic SARS-CoV-2 BTI. Written informed consent was obtained from all participants in accordance with the principles of the Declaration of Helsinki. This study is part of the ORCHESTRA project (Connecting European Cohorts to increase common and Effective SARS-CoV-2 Response) and was approved by the Ethics Committee of the Faculty of Medicine at LMU Munich (20–371).

METHOD DETAILS

Assessment of SARS-CoV-2 strains

SARS-CoV-2 BTI within this cohort occurred from November 2021 to December 2022 and were confirmed by SARS-CoV-2 N-specific seroconversion. For logistical reasons, individuals who reported BTI were sampled only, once they were SARS-CoV-2 negative. The infecting SARS-CoV-2 variant was therefore imputed using the Bavarian Variants of Concern (Bay-VOC) database at weekly resolution and using >50% likelihood of a specific variant as a cutoff (https://www.bay-voc.lmu.de/surveillance.xhtml). This database tracks the sequence of the SARS-CoV-2 VOC using data provided by hospitals and institutes in the region of Bavaria, Germany throughout the pandemic (starting from November 2020).

Pseudovirus neutralization assay

The capacity of sera to neutralize different SARS-CoV-2 variants was determined using a lentiviral pseudotype assay, as described previously.[33,38] In brief, an inoculum of 10^5 rlu/well of lentiviral particles expressing luciferase and pseudotyped with the according variant-specific SARS-CoV-2 spike protein was neutralized with a 2-fold serum dilution series (starting from 1 in 20) for 1 h. Luciferase activity was determined 48 h post infection of HEK293T-ACE2-cells using BrightGlo (Promega Corp, Madison, WI, USA). The 50% inhibitory concentration (IC_{50}) of the

sera was calculated with Prism 8 GraphPad (San Diego, CA, USA) after normalizing to non-infected and infected cells. Magnitude-breadth analysis was performed as described by others.[39] In brief for each serum and time point, a "survival curve" was calculated, with the "event" of interest being neutralization of one variant and the "time-to-event" representing the titer required to get 50% neutralization. Despite data censoring, areas under the curve were calculated to compare different sera or groups, as with three variants, the AUC provided a better estimate than the 50% maximum Magnitude-Breadth.

Binding antibody titers

Serological assays to test for SARS-CoV-2-specific binding antibodies were performed as previously published.[50,52] EDTA plasma was used to quantify binding antibodies specific for S and N protein throughput the study using Roche Elecsys anti-nucleocapsid (Ro-N-Ig) (Roche, Mannheim, Germany). All assays were performed according to manufacturer's instructions. A value above 0.8 counts on the Ro-N-Ig was considered as a positive response towards the SARS-CoV-2 nucleocapsid.

Flow cytometry

PBMCs were isolated within 6 h of blood collection via density gradient centrifugation (Cytiva Sweden AB) and stimulated immediately with peptide pools representing the nucleocapsid, spike and membrane proteins of SARS-CoV-2 (1 μg/ml/peptide, Miltenyi Biotec) for 16 h at 37°C in the presence of anti-CD28 (clone L293, 1 μg/ml, BD Biosciences), anti-CD49d (clone L25, 1 μg/ml, BD Biosciences), and brefeldin A (5 μg/ml, Sigma-Aldrich). Negative control wells lacked stimulants, and positive control wells contained staphylococcal enterotoxin B (SEB, 0.6 μg/ml, Sigma-Aldrich). Cells were then stained with anti-CD4–ECD (clone SFCI12T4D11, Beckman Coulter) and anti-CD8–APC-AF750 (clone B9.11, Beckman Coulter). Labelled cells were fixed and permeabilized using a FoxP3 / Transcription Factor Staining Buffer Set (eBioscience) and further stained intracellularly with anti-CD3–APC-AF700 (clone UCHT1, Beckman Coulter), anti-IFNγ–FITC (clone B27, BioLegend), anti-IL2–PE (clone MQ1-17H12, BioLegend) and anti-TNF-α–BV510 (clone mAb11, BioLegend). Samples were acquired using a CytoFLEX Flow Cytometer (Beckman Coulter). Data analysis was performed using FlowJo software version 10 (FlowJo LLC). Background subtraction was performed by subtracting IFNγ+ T cell frequencies in the negative control from those in the antigen stimulated sample.

QUANTIFICATION AND STATISTICAL ANALYSIS

Statistical modelling

Basic statistical analyses were performed using non-parametric tests in Prism version 8 (GraphPad). For Kaplan-Meier curves the patients that have not completed threefold vaccination and those who were observed for less than 230 days after third vaccination or after BTI, respectively, were excluded from the data used for the curve. The line depicting post third vaccination behaviour is based on 32 individuals, post BTI curve – on 18 subjects. The percentage was calculated with respect to the number of patients meeting the criteria; the R package survival was used for the analysis.[53]

In order to understand the effect of antibodies on reduction of infection risk, Cox regression with proportional hazards assumption was performed with the R survival package (Figures 6 and S5). 95% confidence intervals for hazard ratios were obtained with the R package gtsummary.[54] Here, a hazard ratio below 1 indicates a reduction in hazard by presence of antibodies, CD4$^+$ or CD8$^+$ T cells.

Infection model

To estimate the effect of neutralizing antibodies on the risk of getting infected after three vaccinations against SARS-CoV-2 an infection model was created. For this model, we assumed two states "susceptible" (S) and "infected" (I). We derived the unconditional probability density of becoming infected within time t according to the framework used in standard survival analysis by applying a hazard rate that is tailored to an infection process. Hence, our approach differs from the semi-parametric Cox regression. The time-dependent hazard rate for the infection is assumed to follow the equation:

$$h(t) = \beta_0 \cdot \frac{Incidence\,(t)}{10^5} \cdot (1\; tanh(\beta_1 \cdot log(Antibodies(t))))$$

Here, Incidence(t) is the seven-day incidence per 100,000 inhabitants in Munich at time t (source RKI COVID Datenhub, https://npgeo-corona-npgeo-de.hub.arcgis.com/). The base risk of infection β0 was fixed according to estimates of contact rates from SEIR models 20-22. Additionally, the hazard rate is influenced by the IC$_{50}$ neutralizing antibody titers Antibodies(t) against the SARS-CoV-2 Omicron variant BA.5. The reductive effect of the antibodies on the infection risk is captured by the linear scaling factor β1 in the term 1 – (tanh (β1 × log (Antibodies(t)). Large values of β1 reduce the risk of infection, whereas values close to 0 would indicate no effect. Furthermore, the term tanh (β1 × log (Antibodies(t))) can be used to describe the percent reduction in infection risk conveyed by the neutralizing antibodies. Note that tanh(x) becomes negative if x falls below zero. However, this never occurred in this study. Additionally, we tested our model by replacing tanh with the logistic function and obtained similar results.

We estimated β1 from infection times after three vaccinations of the study volunteers. The neutralizing antibody levels of each individual were estimated beforehand using a linear mixed effects model. Here, we assumed an exponential decay of the antibodies after third vaccination. For estimation of the parameters of the mixed effects model, the R package lme4 was used.[46] The infection model was implemented in julia and the parameters were estimated using the julia interface to the NLopt optimizer library (https://github.com/JuliaOpt/NLopt.jl).[55] After

having estimated the effect of the antibodies, we compared model simulations after third vaccination to the observed data by drawing infection times for each study volunteer from the previously derived infection time distribution. Given these simulations, we calculated the 2.5% and 97.5% simulation quantile at each observed infection time for visualization. With good agreement of model and data, the model was used to predict secondary infections with Omicron BA.5 after BTI for several individuals. Therefore, we used measurements of neutralizing antibodies after BTI, reported COVID-19 cases in Munich and estimates for $\beta 0$ ($\approx$ 11.55) and $\beta 1$ ($\approx$ 0.36), to draw the time of infection within 180 days after BTI for the 30 individuals of this study for 1000 times each from the infection time distribution.

Reduction in viral load by pre-existing nucleocapsid specific T cells

In order to estimate the influence of pre-existing N-specific CD4$^+$ IFNɣ+ T cells, we first estimated the average number of pre-existing T-cells at 180 days after BTI using an exponential decay model. For the estimation, we employed the R package nlme.[56] The model was calibrated on the flow cytometric measurements of CD4$^+$ IFNɣ+ T-cells after BTI assuming a peak response at 14 days after infection. Using this model, the average T-cell concentration could be calculated at 180 days after BTI. At that time a secondary infection was assumed, which would lead to the expansion of T-cells. We tested different expansion factors for seven days after infection. Given the expanded T-cell population at day seven after infection, we used a linear mixed effects model developed by Eser et al. [11] to estimate the reduction in upper airway viral load between two virtual individuals: one with pre-existing N-specific CD4+IFNɣ+ T-cells and one without. For the individual without pre-existing T-cells, the T-cell concentration between day four and seven after symptom onset measured by Eser et al. was used. This measurement was taken to be a baseline T-cell level and added to the expanded T cell concentration of the individual with pre-existing T cells. Then, the model from Eser et al. was evaluated for both virtual individuals and the ratio of viral loads was calculated.